

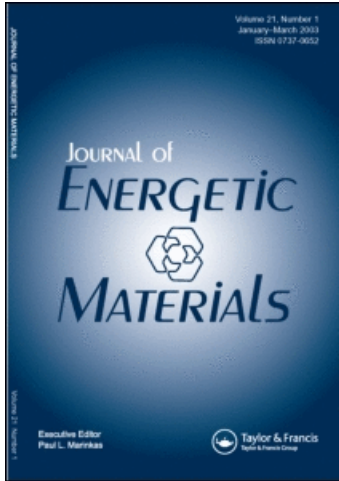
This article was downloaded by:

On: 16 January 2011

Access details: *Access Details: Free Access*

Publisher *Taylor & Francis*

Informa Ltd Registered in England and Wales Registered Number: 1072954 Registered office: Mortimer House, 37-41 Mortimer Street, London W1T 3JH, UK



Journal of Energetic Materials

Publication details, including instructions for authors and subscription information:

<http://www.informaworld.com/smpp/title~content=t713770432>

Constant Strain Criteria for Mechanical Failure of Energetic Materials

Donald A. Wiegand

To cite this Article Wiegand, Donald A.(2003) 'Constant Strain Criteria for Mechanical Failure of Energetic Materials', Journal of Energetic Materials, 21: 2, 109 – 124

To link to this Article: DOI: 10.1080/713845499

URL: <http://dx.doi.org/10.1080/713845499>

PLEASE SCROLL DOWN FOR ARTICLE

Full terms and conditions of use: <http://www.informaworld.com/terms-and-conditions-of-access.pdf>

This article may be used for research, teaching and private study purposes. Any substantial or systematic reproduction, re-distribution, re-selling, loan or sub-licensing, systematic supply or distribution in any form to anyone is expressly forbidden.

The publisher does not give any warranty express or implied or make any representation that the contents will be complete or accurate or up to date. The accuracy of any instructions, formulae and drug doses should be independently verified with primary sources. The publisher shall not be liable for any loss, actions, claims, proceedings, demand or costs or damages whatsoever or howsoever caused arising directly or indirectly in connection with or arising out of the use of this material.

Constant Strain Criteria for Mechanical Failure of Energetic Materials

DONALD A. WIEGAND

Explosives and Warheads Division, ARDEC,
Picatinny Arsenal, NJ, USA

The mechanical response in compression of several explosives was determined as a function of temperature and strain rate. The compressive strength (maximum stress) and the Young's modulus increase with decreasing temperature and increasing strain rate and are proportional to each other. While the compressive strength and Young's modulus vary by about an order of magnitude, the strain at the maximum stress is approximately constant with variations of strain rate and temperature. This approximately constant strain, which can be used as a criteria for failure, is attributed to damage generation that is a function of strain but not temperature or strain rate.

Introduction

This work was initiated to survey the mechanical properties of a group of polymer composite explosives and is expanded here to include other explosives [1–3]. The polymer composites are made up of polymer binders (with plastizer in most cases) and 48–95% organic polycrystalline nonpolymer explosive fillers (see Table 1). One nonpolymer composite, Composition B, and the binder for this composite, TNT, are also considered. The general approach of the work presented was to determine the stress-strain properties of these composites as a function of temperature and strain rate over the ranges of interest. The condition of the samples after deformation was also noted, that is, whether there was evidence of plastic deformation, cracking, and/or fracture.

Address correspondence to D. Wiegand, ARDEC, Picatinny Arsenal, NJ 07806. E-mail: donald.wiegand@us.army.mil

Table 1
Composition of energetic materials interest

Name	Binder			T_{lg} (°C)
	Particulate	Polymer	Plastizer	
Pax 2	HMX 80%	CAB 8%	BDNPA/F 12%	-37 [6]
Pax 2A	HMX 85%	CAB 6%	BDNPA/F 9%	-37 [6]
9404	HMX 94%	NC 2%	CEF 3.84%	-34 [7]
9501	HMX 95%	ESTANE 5703-F1 2.5%	BDNPA/F 2.5%	41(B) [8]
9502	TATB 95%	KEL F 800 5%	30(B) [7]	
LX-14	HMX 95.5%	ESTANE	-31(B) [7]	
Comp B	RDX 59.5%	5702-F1 4.5% TNT/WAX 39.5/1%		
TNT	TNT 100%	NC* 28%	NG 22%	-57 [9,10]
M30	NQ 48%	CAB/NC	BDNPA/F 8%	
M43	RDX 76%	12%/4%		

HMX: cyclotetramethylene tetramine; TATB: 1,3,5-triamino-2,4,6-trinitrobenzene; RDX: cyclotrimethylene trinitramine; NQ: nitroguanidine; TNT: trinitrotoluene; NC: nitrocellulose; NG: nitroglycerine; CAB: cellulose acetate butyrate; BDNPA/F: bis(2,2-dinitropropyl)acetal/formal; CEF: tris(beta chloroethyl)phosphate; Estane: polyurethane; KEL F 800: chlorotrifluoroethylene/vinylidene fluoride copolymer; B: Property of the binder.

*Also contains 2% ethyl centralite.

Experimental

Stress-strain data in compression were obtained using an MTS servo-hydraulic system operated at constant strain rates of 0.001–30/sec [4]. Samples were in the form of right circular cylinders 1.27–2.54 cm in length and 1.27–1.90 cm in diameter. The end faces of the samples were coated with a lubricant, for example, graphite, to minimize frictional effects between the sample and the loading platens. Samples were conditioned at temperatures between -60 and 75°C for at least 2 hr before measurements and were compressed along the cylinder axis to obtain engineering stress and strain. One to five samples were measured at each temperature and strain rate. In most cases measurements were made at four temperatures between -45 and 75°C and at four strain rates between 0.001 and 1.0/sec.

Samples of the polymer composite explosives were prepared either by pressing to size or by pressing into large billets and machining to size [1,2,4,5]. Samples of the two nonpolymer explosives were cast and machined to size [4]. Precautions were taken to ensure that the cylinder end faces were adequately flat and parallel. The densities of all samples were measured. Results are presented only for samples having densities in a narrow range close to the maximum theoretical (zero porosity) density. In Table 1 the major components of the energetic materials considered are given, and the glass transition temperatures, T_g , are given where known.

Results

A typical stress-strain curve for the materials of Table 1 is given in Figure 1. As shown in this figure, the stress initially increases linearly with strain, then curves over and passes through a maximum stress with further increases in strain. The stress either decreases continuously for additional increases in strain beyond the maximum stress at higher temperatures or decreases abruptly to near zero at or just beyond the maximum stress at lower temperatures. Three quantities taken from the stress-strain curves are of interest: the initial slope, which is taken as a measure of Young's modulus, E ; the maximum stress (the compressive strength), σ_m ; and the strain at the maximum stress, ϵ_m .

Linear relationships between σ_m and E and a constant ϵ_m were found for PAX 2, PAX 2A, PBX 9404, PBX 9501, PBX 9502, LX-14, Comp B and TNT (see Table 1) with changes in temperature

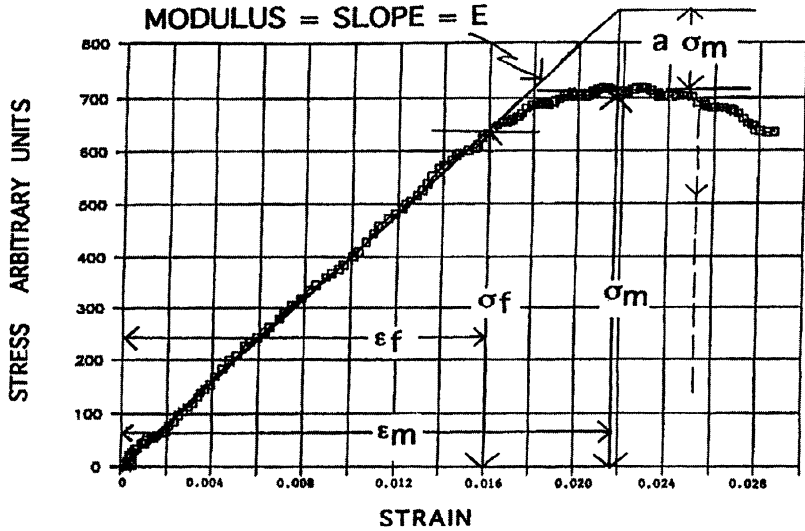


Figure 1. Typical stress-strain response at most temperatures and strain rates for the energetic materials considered. The dashed curve indicates response at low temperatures for some materials.

and strain rate. In addition, the works of Lieb [11], Lieb and Leodore [12], and Gozonas [13,14] indicate that these same relationships are valid for the gun propellant M30 and may also be valid for the gun propellants M14 [11,15] and M43 [11,16]. However, the temperature and strain rate ranges for this linearity between σ_m and E and constant ϵ_m vary with the energetic material. For PBX 9404, PBX 9501, and PBX 9502 (group A) these relationships are valid for approximately the whole measured temperature range from -45 to 75°C , and the whole measured strain rate range from 0.001 – $1.0/\text{sec}$. In contrast, for PAX 2, PAX 2A, and LX-14 (group B) the linear relationship and constant ϵ_m are valid only from approximately 0 to 65°C and the strain rate range given above.

The linear relationship and constant ϵ_m were observed for Comp B and TNT from 20 to 60°C , the only temperature range for which data are available at this time. The strain rate ranges for Comp B and TNT are approximately the same as those given above. These same relationships are valid for the propellant M30 between at least -40 and 50°C and for a range of strain rates [11–14] as well as for the propellants

M14 and M43 for the same temperature range but for one strain rate [11,15–16].

The results are illustrated in Figures 2, 3, and 4 for PBX 9404. σ_m and E change by at least an order of magnitude over the linear range of Figure 2, while the data of Figure 3 indicate that ε_m is approximately constant for these same conditions. The larger scatter in the data of Figure 2 at low temperatures compared to the higher temperatures is associated with increased brittleness at the lower temperatures. The results for the other composites of group A are similar to those of Figures 2 and 3. The results for the other energetic materials are similar to those of Figures 2 and 3 in the temperature and strain rate ranges specified. The relationships between σ_m , E , and ε_m for this latter group of energetic materials outside of the temperature and strain rate ranges specified are considered elsewhere [17].

From Figure 1 the relationship between the three quantities σ_m , E and ε_m is found to be

$$\sigma_m = \frac{E\varepsilon_m}{1+a}, \quad (1)$$

where a is a measure of the shape of the stress-strain curve between the point where it deviates from the initial straight line and the

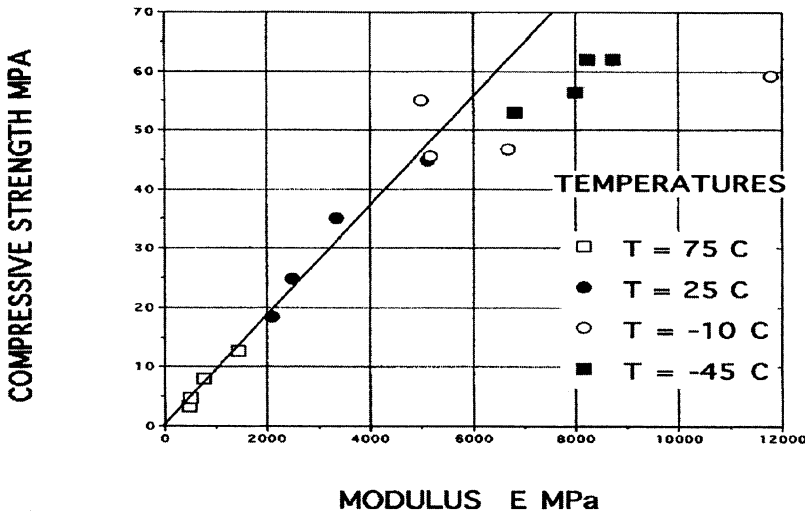


Figure 2. Compressive strength (σ_m) versus E for PBX 9404.

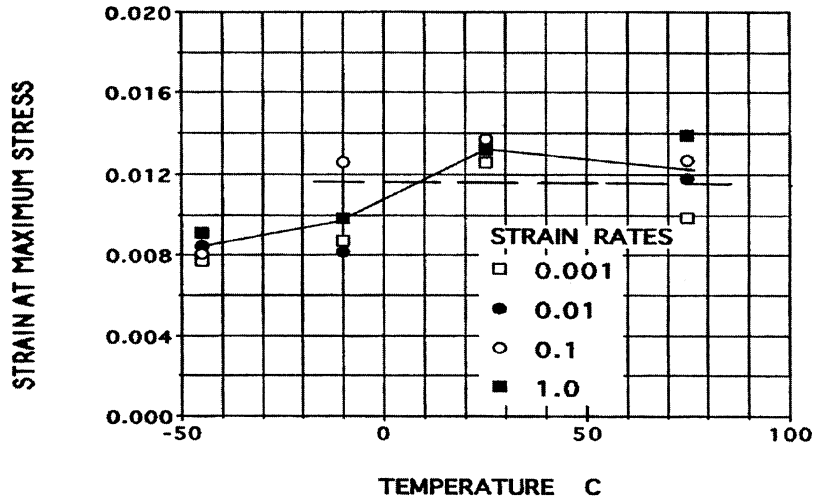


Figure 3. Strain (ϵ_m) at the maximum stress versus temperature for PBX 9404.

point of maximum stress. A linear relationship between σ_m and E and a constant ϵ_m then requires $(1 + a)$ to be constant to satisfy this equation. Although the parameter a does change somewhat with temperature, the magnitudes and changes in a are such that equation (1) is satisfied by data of the type seen in Figures 2 and 3 for all of the materials of the table within the precision of the measurements and within the temperature and strain rate limits given above.

A measure of the damage introduced by deformation can be obtained by studies of Young's modulus as a function of prior strain. The uniaxial stress-strain behavior after prior uniaxial deformation indicates that for maximum prior strains in the initial linear region of the stress-strain curve (Figure 4), a change in the modulus is not detected. However, for maximum prior strains beyond this linear range the modulus decreases continuously with increasing prior maximum strain and so amount of damage [18,19]. This is shown in Figure 5. ϵ_f (Figure 1) is taken as a measure of the strain required for the initiation of modulus reduction by damage generation. The stress-strain response can be considered as determined by the locus of points fixed by the strain, the modulus at that strain, and the permanent strain. The permanent strain remaining after prior

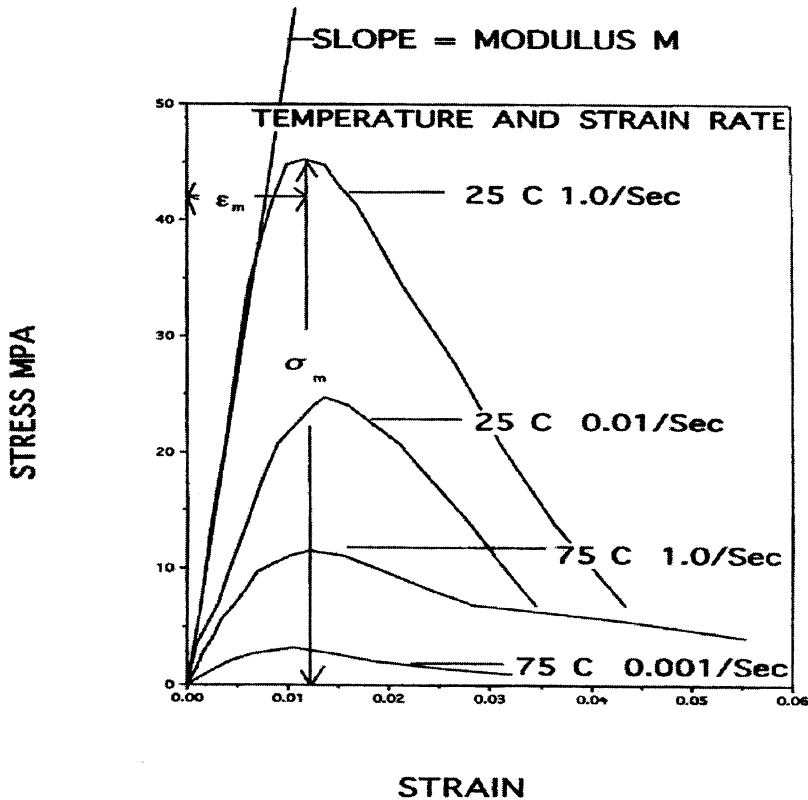


Figure 4. Stress-strain curves in uniaxial compression for PBX 9404 for various conditions of temperature and strain rate.

strain also increases with the amount of prior strain, as shown in Figure 5.

At the lowest temperatures all polymer composites give evidence of abrupt fracture, that is, an abrupt decrease of the stress with increasing strain at strains equal to or greater than the strain at the maximum stress (see Figure 1). In addition, at the lowest temperatures PAX 2, PAX 2A, M30 [9,10], and M43 [11] fracture-fragment into many pieces, whereas PBX 404, PBX 9501, PBX 9502, and LX-14 fracture into several pieces. Therefore, most of the group that fragment into many pieces at low temperatures do not have a constant strain and σ_m proportional to E in the low-temperature range (group

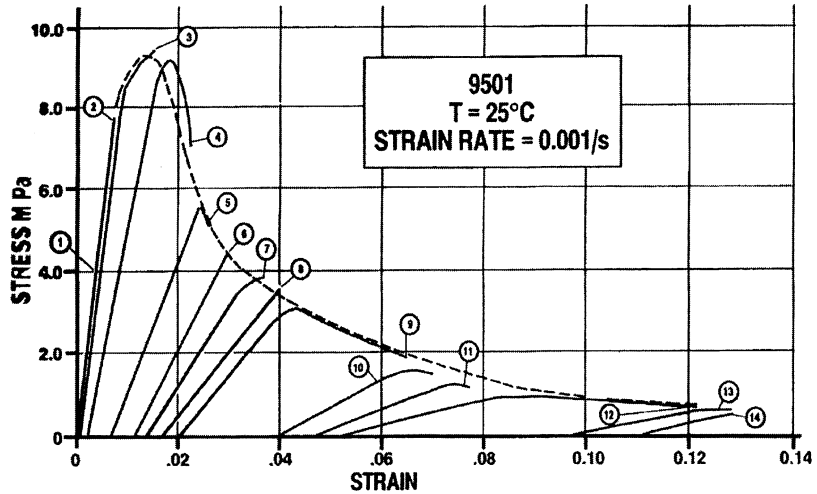


Figure 5. Series of stress-strain curves for one sample taken in the sequence indicated by the circled numbers. For each solid curve the stress was increased to the final value and then reduced to zero (the latter is not shown). Each curve is offset from the origin by the permanent strain from the previous curve, measured several hours later. The dashed curve was taken for a separate sample without interruption. Data are for PBX 9501.

B), whereas most of the group that fracture but do not fragment do have a constant strain and σ_m proportional to E over most of the temperature range (group A).

At the highest temperatures, in contrast, all polymer composites deform extensively in a plastic-like manner and do not show the abrupt decrease of stress with increasing strain. At the highest temperatures PAX 2, PAX 2A, M30, and M43 [11] exhibit some cracking at very large strains, while PBX 9404, PBX 9501, PBX 9502, and LX-14 tend to fracture at large strains. The transition from the low- to high-temperature behavior is gradual with increasing temperature and is somewhat strain rate dependent. PBX 9502, which has a significantly higher T_g than the others, shows the transition from the low- to high-temperature behavior at a higher temperature. Data are not available in the low-temperature range for Comp B and TNT, but at the higher temperatures these materials fracture into several pieces without giving evidence of extensive plastic deformation [4].

Discussion

The results presented above concerning the modulus decrease with increasing prior strain indicate that the uniaxial stress-strain response can be expressed as

$$\sigma = E\varepsilon = (E_o - \Delta E)\varepsilon \quad (2a)$$

$$= \frac{\varepsilon}{Y} = \frac{\varepsilon}{Y_o + \Delta Y}, \quad (2b)$$

where E is Young's modulus, Y is the compliance, E_o and Y_o are the values before damage due to loading, and ΔE and ΔY are the changes due to damage introduced by loading. To first order, $\Delta E/E_o = \Delta Y_o$. ΔY is assumed to be a single-valued monotonically increasing function of ε . Y_o and ΔY may be functions of temperature, strain rate, initial crack, and dislocation parameters, density, etc. However, all damage, for instance, changes in crack and dislocation parameters, are assumed to be expressed through the dependence of these changes on ε . Dienes [20] and Dienes and Riley [21] used equation (2) and several models for the dependence of ΔY on crack parameters in fitting this author's data for PBX 9501 (see below).

The condition for a maximum in the curve of σ versus ε is found from equation (2b) to be

$$\varepsilon_m = \frac{Y_o + \Delta Y_m}{\Delta Y'_m}, \quad (3)$$

where the subscript m denotes the values at the maximum and the prime symbol indicates differentiation with respect to ε . The stress at the maximum is

$$\sigma_m = \frac{1}{\Delta Y'_m}. \quad (4)$$

From equation (3) $\Delta Y'_m$ must be nonzero and positive. Thus, ΔY_m must be an increasing function of ε , as assumed. A linear relationship between σ_m and E_o is obtained if $\Delta Y'_m$ is expressed as

$$\Delta Y'_m = Y_o f(\varepsilon_m)' = \frac{f(\varepsilon_m)'}{E_o}, \quad (5)$$

with $f(\varepsilon_m)'$ independent of temperature and strain rate. It is assumed here that the initial linear slope of the stress-strain curve is given by E_o . Substitution of equation (5) into equation (3) yields

$$\varepsilon_m = \frac{Y_o + \Delta Y_m}{Y_o f(\varepsilon_m)'}. \quad (6)$$

If

$$\Delta Y_m = Y_o f(\varepsilon_m), \quad (7)$$

ε_m is independent of temperature and strain rate in agreement with experiment. Thus, the relationships for σ_m and ε_m are

$$\sigma_m = \frac{E_o}{f(\varepsilon_m)'} \quad (8a)$$

and

$$\varepsilon_m = \frac{1 + f(\varepsilon_m)}{f(\varepsilon_m)'}, \quad (8b)$$

where $f(\varepsilon_m)$ and $f(\varepsilon_m)'$ are independent of temperature and strain rate.

If $f(\varepsilon)$ is expressed as a power series in ε , the condition for a maximum in the σ versus ε curve is that the highest power of ε is greater than unity. The total compliance from equations (2) and (7) is then given by

$$Y = Y_o(1 + f(\varepsilon)), \quad (9)$$

so that

$$(1 + f(\varepsilon)) \quad (10)$$

is a damage function for the compliance. However, it must be emphasized that the development leading to equations (7)–(10) is valid only for the initial part of the stress-strain curve up to and including the maximum. The form of the damage function in the work softening region will be addressed separately [22].

In summary, by expressing the total compliance as the sum of the undamaged compliance and the change in compliance due to damage, and by comparing the resulting equations for σ_m and ε_m with the experimental results, it is concluded that the change in compliance is proportional to the undamaged compliance (equation (7)), and further that the damage function is a function of the total strain and is independent of temperature and strain rate.

The damage approach provides a rational assessment for a constant strain criteria for failure with changes in temperature and strain rate (equation 8b) based on a damage function that is independent of these two parameters in the initial stages of damage (equation 10). In addition, the linear relationship between σ_m and E_o is obtained (equation 8a). Therefore, this damage approach satisfies the experimental criteria. This approach, of course, also provides the rationale for why σ_m has the same temperature and strain rate dependencies and thus activation energy as E_o [19]. The temperature and strain rate dependencies of E_o are thought to be due primarily to the viscoelastic properties of the binder. However, independent of the type of material, the failure strain will be constant with variations of temperature, strain rate, and other parameters if the damage function that is dependent on strain is independent of these other quantities. Dienes refers to other types of materials that exhibit a constant failure strain [20].

As noted above, results indicate that if the strain does not exceed a strain of about ε_f (see Figure 1), a change in the modulus, within the precision of the measurements, is not detected. However, if ε_f is exceeded, the modulus is decreased. [18,19]. Therefore, the damage function (equation 10), at least for practical purposes, has a strain threshold of ε_f . The threshold stress (Figure 1), σ_f , then varies as the modulus with changes in temperature and strain rate, if ε_f is independent of these parameters. Here ε_m and σ_m are taken as measures of ε_f and σ_f .

Although additional work is necessary to establish the nature of the damage, the conclusions that the change in compliance is proportional to the undamaged compliance and that the damage function is independent of temperature and strain rate place restrictions on the possibilities. Thermally activated crack growth apparently is not a possibility because the function $f(\varepsilon)$ (equation (7)) is not a function of temperature or strain rate [4,23]. Fracture of particulate particles, perhaps by particle-particle interactions, under some circumstances may satisfy the necessary conditions. Evidence for decreased

particulate particle sizes of several of the composites of the table after damage by uniaxial compression were found by small angle X-ray and neutron scattering [24]. Although the author is unaware of mechanical property measurements for any of the energetic materials of Table 1 as a function of particulate particle size, measurements were made of pressed HMX, the particulate for most of the composites of Table 1, for two different average particle sizes [25]. Samples containing only coarse HMX gave moduli and compressive strengths higher by about 30% compared to samples containing a bimodal mixture of coarse and fine particles sizes in the ratio 3:1. Both sample groups were pressed to approximately the same density. In contrast, measurements of samples of an inert stimulant of PBX 9501 containing sucrose in place of HMX and with the same two particle size distributions as for the HMX did not show differences in the moduli or the compressive strengths [26]. Measurements of the moduli and the particle sizes for the composites of the table as a function of deformation are desirable.

There have been a few attempts to model the stress-strain curves of the polymer composites under consideration. These models give some insight into the possible processes that may be important in these materials and are reviewed briefly here. Dienes and Riley [21] have assumed that the total change in compliance is due to crack growth and have used equation (2) with Y expressed in the form of equation (9). They have used $f(\varepsilon) = k\varepsilon^3$, as obtained from a very simple crack propagation model, to fit this author's data for PBX 9501 for a range of temperatures and strain rates. Y_o , (E_o), and k were varied to give the best fits to the stress-strain curves for strains between zero and 0.04, the latter being well into the softening region of the curves.

The fits to the data by k and E_o dependent on temperature and strain rate are surprisingly good considering the simplicity of the model. However, the model predicts a much stronger dependence of k on strain rate than obtained by fitting to the data. Although the fits to the initial portions of the stress-strain curves of immediate concern here in several cases are not as good as might be desired, the fitting was optimized for a significantly larger range of strains. The model predicts ε_m to be dependent on k and so strain rate. This is contrary to observations. In addition, the model predicts σ_m to be proportional to E_o as observed, but predicts σ_m to be dependent on k . The strain rate dependence of σ_m because k is a function of strain rate is also contrary to observations.

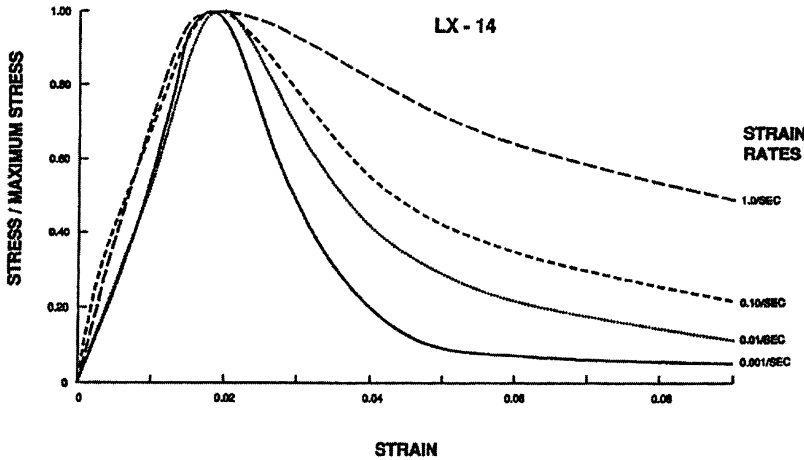


Figure 6. Stress-strain curves for LX-14 normalized to the stress at the maximum.

Experimental stress-strain curves normalized to the maximum stress, that is, σ/σ_m versus ε , are insensitive to temperature and strain rate for the initial parts of the curves but are temperature and strain rate dependent in the softening region (for example, see Figure 6). A more complex model may then be necessary to fit the data in the initial regions and the softening region. The results also indicate that in some cases at higher temperatures there is significant plastic deformation without evidence of cracking. Therefore a more complex model is also required to account for this behavior.

Dienes and Riley fit some of this author's PBX 9501 data to a more complex crack model with realistic crack parameters, but the fits are not as good as the fits with the simpler model [21]. These authors unfortunately used a form of the data for all of their curve fitting that was not corrected for measuring system compliance. This correction influences the data primarily at lower temperatures (larger stresses).

Although Dienes and Riley have neglected the viscoelastic properties of the binder, Aidun has developed a phenomenological viscoelastic model for PBX 9501 based on Maxwell elements [27]. A damage function was deduced to account for the difference between this author's PBX 9501 data at 25°C and the viscoelastic model. Reasonably good fits were obtained over essentially the entire

stress-strain curves by using a damage function that is strain rate independent in the initial parts of the curves up to about the maxima (see Figure 1) but that is strain rate dependent in the softening region at greater strains. This is consistent with the observations that the normalized stress-strain curves are independent of strain rate for the initial range up to the maximum stress but are strain rate dependent for greater strains in the softening region, as shown in Figure 6. This strain rate dependence of the damage function is also consistent with the above discussion of the parameter k used by Dienes and Riley [21]. Temperature variations were not considered by Aidun.

In addition, Gozonas has developed a nonlinear viscoelastic model with damage due to crack growth that he has fitted to M30 propellant data as a function of temperature and strain rate for strains in the vicinity of and greater than ε_m [13,14]. By fitting the model to the constant strain rate stress-time data at the two extremes of strain rate and at a given temperature, he has shown that the model correctly predicts the stress versus time data at two intermediate strain rates. The model gives a constant ε_m and correctly predicts other features of the data including the observed dependence of σ_m on strain rate. The model also indicates that the damage function is constant at ε_m as strain rate changes. However, the model does not appear to fit the data very well in the initial increasing stress portion of the stress-time and so the stress-strain curves, and so the observed moduli and the linear relationship between the modulus and the compressive strength are not predicted.

A linear relationship between the modulus and the tensile yield strength has been observed and predicted for glassy polymers at very low temperatures [28,29]. The proportionality constant between the tensile yield strength and the modulus is found to be approximately 0.019–0.13. In comparison, the proportionality constant between the compressive strength and the modulus is approximately 0.009–0.05 for the polymer composites studied here. However, the results presented here are for polymer- particulate composites primarily above T_g .

Although the modeling work reviewed above indicates that there has been significant progress in attempting to predict results of the type presented in this paper, it is also apparent that even more complex models may be necessary to describe the stress-strain behavior for the full range of temperatures and strain rates for which the failure strain is constant.

Summary

Several explosives were studied in uniaxial compression over a range of temperatures and strain rates. The results indicate that the strain at the maximum stress, taken as a measure of the failure strain, is constant over a significant range of temperatures and strain rates. In addition, the maximum stress, the compressive strength, is proportional to Young's modulus over this same range of temperatures and strain rates. This proportionality is shown to be expected from geometrical considerations when the failure strain is constant. The results also indicate that Young's modulus decreases continuously with increasing prior strain and so damage, after a threshold strain. The constant failure strain is attributed to damage generation that is a function only of strain and thus not a function of temperature or strain rate. The damage is manifested as a decrease in Young's modulus and thus an increase in compliance after prior strain. It may be more convenient in some circumstances to consider failure conditions in terms of a constant failure strain rather than a failure stress that is a function of temperature and strain rate.

Acknowledgments

Thanks are due to R. Lieb for providing propellant mechanical properties data in tabular form. The author also wishes to acknowledge the assistance of C. Hu with measurements. This work was supported in part by Sandia National Laboratories, Albuquerque, New Mexico.

References

- [1] Wiegand, D., C. Hu, A. Rupel, and J. Pinto. 1994. *9th International Conference on Deformation, Yield and Fracture of Polymers*. London: Institute of Materials, pp. 64/1–64/4.
- [2] Wiegand, D. A. 1995. *3rd International Conference on Deformation and Fracture of Composites*, University of Surrey, Guildford, U.K., pp. 558–567.
- [3] Wiegand, D. A. 1996. *Proceedings of the 20th Army Science Conference*, Norfolk, VA, vol. 1, p. 63.
- [4] Wiegand, D. A., J. Pinto, and S. Nicolaides. 1991. *J. Energetic Materials*, 9: 19.
- [5] Wiegand, D. A. 1994. *Materials Research Society Symposium Proceedings, Interface Control of Electrical, and Mechanical Properties*, ed. S. P. Murarka, K. Rose, T. Ohmim, and T. Seidel, vol. 318, pp. 387–392.

- [6] Harris, J. Private communication.
- [7] Dobratz, B. M., and P. C. Crawford. 1985. *LLNL Explosives Handbook, Properties of Chemical Explosives and Explosive Simulants*, Lawrence Livermore National Laboratory Report UCRL-52997 Change 2, p. 6-6 and p. 6-8.
- [8] Flowers, G. L. Private communication.
- [9] Nicolaides, S., J. Pinto, and D. A. Wiegand. 1980. Chemical Propulsion Information Agency Publication 315.
- [10] Nicolaides, S., D. A. Wiegand, and J. J. Pinto. 1982. Picatinny Arsenal Technical Report, ARCLD-TR-82010, Picatinny Arsenal, NJ.
- [11] Lieb, R. Private communication.
- [12] Lieb, R. J., and M. G. Leadore. 1993. ARL-TR-307, Army Research Laboratory, Aberdeen Proving Grounds, MD. November.
- [13] Gazonas, G. A. 1993. *Mechanics of Materials*, 15: 323, and Technical Report ARL-TR-115. April.
- [14] Gazonas, G. A. 1994. Technical Report ARL-TR-469. June.
- [15] Lieb, R. 1996. ARL-TR-1205, Army Research Laboratory, Aberdeen Proving Grounds, MD.
- [16] Lieb, R. J. 1995. ARL-TR-884, Army Research Laboratory, Aberdeen Proving Ground, MD. October.
- [17] Wiegand, D. A. 1998. Picatinny Arsenal Technical Report ARWEC-TR-98008. November.
- [18] Wiegand, D. A. 1996. *Bull. Am. Phys. Soc.*, 41(1): 676.
- [19] Wiegand, D. A. 1998. *Proceedings of the 11th International Detonation Symposium*, Snowmass, CO, p. 744.
- [20] Dienes, J. K. Los Alamos National Laboratory Report LA-UR-98-3620.
- [21] Dienes, J. K., and N. R. Riley. Los Alamos National Laboratory Report LA-UR-98-3804.
- [22] Wiegand, D. A. to be published.
- [23] Wiegand, D. A. 1997. *Bull. Am. Phys. Soc.* 42(1): 97.
- [24] Trevino, S. F., and D. A. Wiegand. 1998. *Proceedings of the 21st Army Science Conference*, Norfolk, VA, p. 181.
- [25] Idar, D. J., P. D. Peterson, C. S. Fugard, and G. T. Gray. 1997. Twentieth Semiannual Meeting of TCG1, Lawrence Livermore National Laboratory, December, and private communication.
- [26] Idar, D. J., P. D. Peterson, P. D. Scott, and D. J. Funk. 1997. Los Alamos National Laboratory Report LA-UR-97-2641, and *Proceedings of the American Physical Society Topical Conference on Shock Compression of Condensed Matter*, ed. S. C. Schmidt, D. P. Dandekar, and J. W. Forbes, p. 587.
- [27] Aidun, J. Unpublished report and private communication.
- [28] Bowden, P. B., and S. Raha. 1974. *Phil. Mag.*, 77: 150.
- [29] Argon, A. S., and M. I. Bessonov. 1977. *Phil. Mag.*, 35: 917.